

See discussions, stats, and author profiles for this publication at: <https://www.researchgate.net/publication/45514931>

Zeolithic Imidazolate Frameworks as H₂ Adsorbents: Ab Initio Based Grand Canonical Monte Carlo Simulation

ARTICLE in THE JOURNAL OF PHYSICAL CHEMISTRY C · JULY 2010

Impact Factor: 4.77 · DOI: 10.1021/jp103785u · Source: OAI

CITATIONS

37

READS

31

5 AUTHORS, INCLUDING:



Sang Soo Han

Korea Research Institute of Standards and ...

58 PUBLICATIONS 1,900 CITATIONS

[SEE PROFILE](#)



Seung-Hoon Choi

Insilicotech Co.

40 PUBLICATIONS 687 CITATIONS

[SEE PROFILE](#)



William A. Goddard

California Institute of Technology

1,345 PUBLICATIONS 68,927 CITATIONS

[SEE PROFILE](#)

Zeolitic Imidazolate Frameworks as H₂ Adsorbents: Ab Initio Based Grand Canonical Monte Carlo Simulation

Sang Soo Han,^{*,†} Seung-Hoon Choi,[‡] and William A. Goddard III[§]

Center for Nanocharacterization, Korea Research Institute of Standards and Science, 209 Gajeong-Ro, Yuseong-Gu, Daejeon 305-340, Republic of Korea, Insilicotech Company Limited, A-1101 Kolontripolis, 210, Geumgok-Dong, Bundang-Gu, Seongnam, Gyeonggi-Do 463-943, Republic of Korea, and Materials and Process Simulation Center (MC 139-74), California Institute of Technology, Pasadena, California 91125

Received: April 27, 2010; Revised Manuscript Received: June 1, 2010

We report the H₂ uptake behavior of 10 zeolitic-imidazolate frameworks (ZIFs), based on grand canonical Monte Carlo (GCMC) simulations. The force fields (FFs) describing the interactions between H₂ and ZIF in the GCMC were based on ab initio quantum mechanical (QM) calculations (MP2) aimed at correctly describing London dispersion (van der Waals attraction). Thus these predictions of H₂ uptake are based on first principles (non empirical) and hence applicable to new framework materials for which there is no empirical data. For each of these 10 ZIFs we report the total and excess H₂ adsorption isotherms up to 100 bar at both 77 and 300 K. We report the hydrogen adsorption sites in the ZIFs and the relationships between H₂ uptake amount, isosteric heat of adsorption (Q_{st}), surface area, and free volume. Our simulation shows that various ZIFs lead to a variety of H₂ adsorption behaviors in contrast to the metal-organic frameworks (MOFs). This is because ZIFs leads to greater diversity in the adsorption sites (depending on both organic linkers and zeolite topologies) than in MOFs. In particular, the ZIFs uptake larger amounts of H₂ at low pressure because of the high H₂ adsorption energy, and ZIFs have a variety of H₂ adsorption sites. For example, ZIF-11 has an initial Q_{st} value of ~15 kJ/mol, which is higher than observed for MOFs. Moreover, the preferential H₂ adsorption site in ZIFs is onto the organic linker, not nearby the metallic joint as is the case for MOFs.

Introduction

Pollution-free, highly abundant, and highly efficient hydrogen has been considered one of the most attractive renewable energy sources. Hydrogen could be used in vehicles and portable electronics as an energy carrier. However, to be useful in the applications, a safe and efficient hydrogen storage medium is needed. In 2009, the United States Department of Energy (DOE) posted new targets for the hydrogen storage capacity: 4.5 wt % and 28 kg/m³ below 100 atm and near room temperature by 2010 and 5.5 wt % and 40 kg/m³ by 2015.¹ An important consideration is that there be no significant barrier to storing and removing the H₂. A number of materials including metal hydrides (e.g., Mg₂Ni, LaNi₅, etc.),² chemical hydrides (e.g., NH₃BH₃),³ nanotubes,⁴ and exfoliated graphites⁵ have been considered for hydrogen storage, but none has been shown experimentally to meet the DOE target yet. The metal hydrides and chemical hydrides have sufficient storage capacity, but these cases involve dissociation of the H₂ upon storage and reformation of the H₂ upon removal, with barriers too large for practical use. The other materials have the advantage that no dissociation and reassociation of the H₂ is required.

Metal-organic framework (MOF) materials, which are composed of metallic joints (e.g., Zn₄O(CO₂)₆) and organic linkers (e.g., 1,4-benzenedicarboxylate), exhibit exceptional porosity, which stimulated many studies to investigate the utility for using these materials as a H₂ adsorbent.⁶ However, without

metal additives, the best experimental performance of an MOF is 1.01 wt % (excess) and 2.30 wt % (total) at 95 bar and 298 K for Be₁₂(OH)₁₂(1,3,5-benzenetribenzoate).⁶ⁱ Theory⁷ predicted that Li-doped MOFs could lead to dramatically improved performance, 5.16 wt % (excess) and 6.47 wt % (total) at 100 bar and 300K for Li-MOF-C30.^{7a} Indeed experiments⁸ performed at 77 K showed that Li doping enhances H₂ storage capacity. This could be a promising and practical option for hydrogen storage, but such metal-doped MOFs have poor stability, resulting in disruption of the network of the MOF upon exposure to humid air.⁹

Recently, the Yaghi group in UCLA synthesized a new class of porous crystals, involving a zeolitic imidazolate framework (ZIF). They did this by copolymerizing Zn(II) or Co(II) with imidazolate-type linkers.¹⁰ ZIF has both a high porosity and an exceptional chemical stability, in contrast to the MOFs. Indeed, the ZIF-8 retains its structure even after 7 days in boiling water.^{10a} This exceptional stability is due to the stable bonding between the nitrogen in imidazolate linkers and Zn(II)/Co(II) and to hydrophobic pore properties.^{10a} This superior stability of ZIFs over MOFs would allow greater versatility when modifying their structure, such as by alkali-metal doping, to improve hydrogen uptake.

Another interesting structural feature of ZIFs is that they have both large pores (11.6 Å for ZIF-8 and 14.6 Å for ZIF-11) and small apertures (3.4 Å for ZIF-8 and 3.0 Å for ZIF-11).^{10a} The sizes of the small apertures are similar to the kinetic diameter (2.9 Å) of H₂, permitting the H₂ to penetrate into the large pore of ZIFs, the hydrogen molecules but the small apertures might exclude other larger molecules. We find that the maximal attraction of a H₂ molecule to the ZIF occurs when the apertures (or pores) are the same size as the kinetic diameter of H₂.^{7g}

* To whom correspondence should be addressed. E-mail: sangsoo@kriss.re.kr.

[†] Korea Research Institute of Standards and Science.

[‡] Insilicotech Company Limited.

[§] California Institute of Technology.

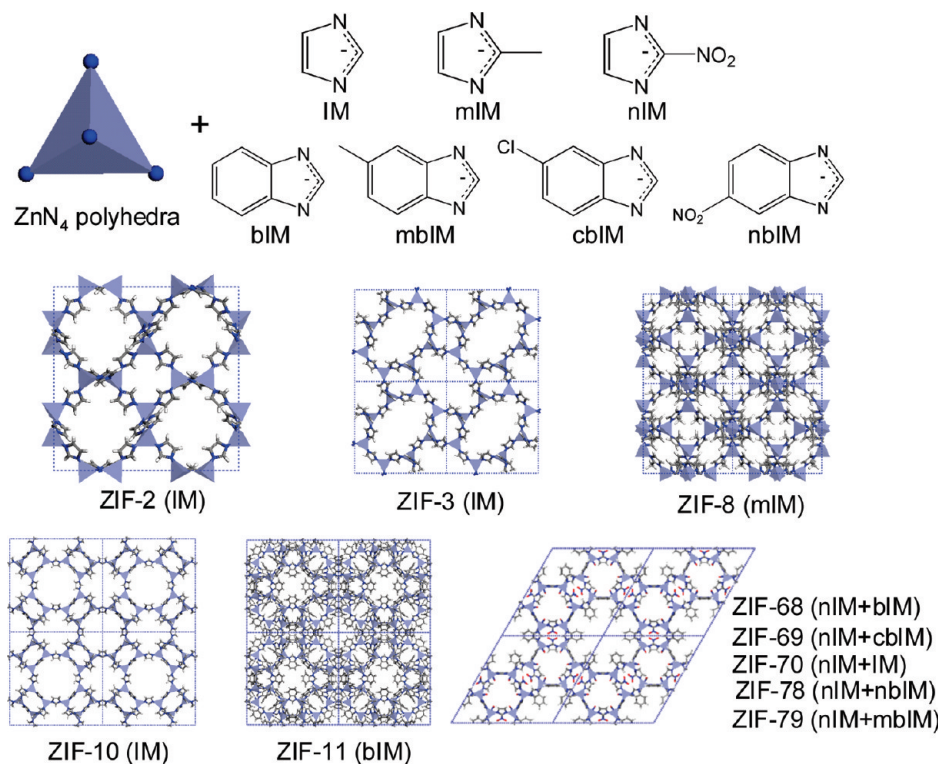


Figure 1. Structures of ZIFs considered in this work. The ZIFs are obtained by combinations of the ZnN_4 polyhedra and imidazolate linkers.

Thus, H_2 adsorption onto ZIFs should display a loading curve behavior different than that of MOFs. In particular, because of the small size of the aperture, the H_2 binding energy around the ZIF aperture is higher than around MOF pores, leading to a higher H_2 uptake at low pressure. This leads to improved performance for practical applications. Indeed, according to experiment,^{10a} ZIF-11 has a smaller aperture size than ZIF-8 leading to a higher H_2 uptake up to 1 bar at 77 K for ZIF-11 than for ZIF-8.

Despite these interesting structural features of ZIFs, few studies on this class of materials have been reported, with most reports limited to ZIF-8. Yaghi and co-workers first reported experimental observations of H_2 uptake in ZIF-8 and ZIF-11 at 77 K, where they considered both low (up to 1 bar) and high (up to 80 bar) pressure cases for ZIF-8 but only the low (up to 1 bar) pressure case for ZIF-11.^{10a} After the experiments by the Yaghi group, Zhou et al. at NIST experimentally measured the total, excess, and effective H_2 adsorption isotherms of ZIF-8 up to 60 bar at several temperatures.¹¹ They also characterized the H_2 adsorption site in ZIF-8 from its neutron diffraction patterns at 3.5 K, where the preferential H_2 adsorption site is nearby the organic linkers, not the ZnN_4 tetrahedra (metal sites), which is in contrast to the MOFs.¹² The Yaghi group also synthesized ZIF-20 and reported H_2 adsorption isotherms up to 1 bar at 77 and 87 K.^{10b}

Some theoretical studies of H_2 uptake in ZIF-8 have been reported. Using an empirical force field (FF) in grand canonical Monte Carlo simulations (GCMC), Zhou et al.¹³ simulated the H_2 adsorption isotherm of ZIF-8 at 77 K and pressures up to 80 bar. Also, they reported the location of the H_2 adsorption sites: the first adsorption site is on both sides of the imidazolate ring (close to the imidazolate $\text{C}=\text{C}$ bond) with the second adsorption site being the pore channel. This is similar to the neutron diffraction pattern results of the Yildirim group.¹²

Liu et al.¹⁴ reported GCMC simulations using DREIDING FF to simulate the H_2 adsorption isotherms of ZIF-8 up to 60

bar at 125, 200, and 300 K. At 300 K, the GCMC simulation shows a good agreement with an experiment (e.g. at 50 bar GCMC leads to ~ 0.35 wt % H_2 while experiment¹¹ leads to 0.33 wt %). However at low temperature the GCMC overestimates the binding (e.g. at 125 K GCMC leads to ~ 2.37 wt % H_2 compared to the experimental result of 2.23 wt %).

In addition, Fischer et al.¹⁵ used several empirical FFs in GCMC studies on ZIF-8 at 77 K. At low pressure (< 1 bar), they found that the best agreement with experiment^{10a} for DREIDING FF (~ 1.30 wt % at 1 bar compared to experiment of ~ 1.25 wt %), while at high pressure (up to 35 bar) they found UFF to be best (~ 3.30 wt % at 35 bar compared to experiment¹¹ of 3.27 wt %).

Using an empirical FF with GCMC methodology, Rankin et al.¹⁶ reported H_2 adsorption isotherms for ZIF-68 and ZIF-70 at 298 K and up to 95 bar. They found that ZIF-68 has a higher excess H_2 uptake amount than ZIF-70, but the amount is very low (~ 0.25 wt % at 77 K and 90 bar).

In order to better understand the effects of functional groups ($-\text{C}_6\text{H}_3\text{Cl}$, $-\text{C}_6\text{H}_3\text{CH}_3$, $-\text{C}_6\text{H}_3\text{NO}_2$, and $-\text{C}_6\text{H}_4$) in ZIFs on hydrogen storage, we report here the H_2 adsorption in ZIFs for 10 different ZIFs (ZIF-2, ZIF-3, ZIF-8, ZIF-10, ZIF-11, ZIF-68, ZIF-69, ZIF-70, ZIF-78, and ZIF-79). Our simulations use FF based on first-principles QM, so we can expect them to be reliable for systems not yet studied experimentally. We report here the H_2 adsorption isotherms (both the total and excess amounts) up to 100 bar at 77 and 300 K. We then analyze the H_2 adsorption sites and the relationships between H_2 uptake amount and the isosteric heat of adsorption, surface area, and free volume.

Computational Details

To date, a number of ZIFs with varying pore size, aperture size, and zeolite topology have been experimentally investigated.¹⁰ On the basis of their aperture size and zeolite topology, we selected the 10 ZIFs shown in Figure 1 for our studies. Their

TABLE 1: Structural Characteristics of ZIFs Considered in This Work

ZIF	composition	zeolite topology ^a	density, g/cm ³	pore diameter, Å ^a	pore aperture diameter, Å ^a	surface area, m ² /g ^b	pore volume, cm ³ /g ^b
ZIF-2	Zn(IM) ₂	BCT	0.929	6.9	6.4	2587 ^c (2077) ^d	0.683 ^c (0.673) ^d
ZIF-3	Zn(IM) ₂	DFT	0.880	6.0	4.6	2810 (2325)	0.757 (0.751)
ZIF-8	Zn(mIM) ₂	SOD	0.925	11.6	3.4	1887 (1539)	0.629 (0.618)
ZIF-10	Zn(IM) ₂	MER	0.746	12.1	8.2	3019 (2647)	0.959 (0.949)
ZIF-11	Zn(bIM) ₂	RHO	1.002	14.6	3.0	1718 (1335)	0.568 (0.558)
ZIF-68	Zn(bIM)(nIM)	GME	1.033	10.3	7.5	1972 (1557)	0.560 (0.552)
ZIF-69	Zn(cbIM)(nIM)	GME	1.149	7.8	4.4	1938 (1515)	0.471 (0.462)
ZIF-70	Zn(IM) _{1.13} (nIM) _{0.87}	GME	0.935	15.9	13.1	1994 (1821)	0.700 (0.691)
ZIF-78	Zn(nbIM)(nIM)	GME	1.175	7.1	3.8	1914 (1378)	0.447 (0.438)
ZIF-79	Zn(mbIM)(nIM)	GME	1.073	7.5	4.0	1879 (1473)	0.500 (0.489)

^a From refs 10c and e. ^b Calculated by Cerius2 software. ^c By H₂ kinetic diameter (2.90 Å). ^d By N₂ kinetic diameter (3.68 Å).

structural properties are summarized in Table 1. When the aperture size of the ZIF is smaller than the kinetic diameter (2.9 Å) of H₂, we expect that the ZIF pores would be kinetically inaccessible for H₂ gas. This would lead to significant discrepancy between simulation and experiment results. Thus, we only considered ZIFs with an aperture size greater than 2.9 Å. In addition, we considered five different zeolite topologies: **BCT** for ZIF-2, **DFT** for ZIF-3, **SOD** for ZIF-8, **MER** for ZIF-10, **RHO** for ZIF-11, and **GME** for ZIF-68, ZIF-69, ZIF-70, ZIF-78, and ZIF-79. Five **GME** ZIFs were selected for studying the effect of functional groups ($-C_6H_3Cl$, $-C_6H_3CH_3$, $-C_6H_3NO_2$, and $-C_6H_4$) on H₂ uptake. All ZIFs considered have the same transition element (Zn).

We simulated the H₂ adsorption isotherms (both the total and excess amount) of the 10 ZIFs from 0 to 100 bar at 77 and 300 K using GCMC simulations. To obtain an accurate measure of H₂ loading, we considered 2×10^6 configurations to compute the average loading for each condition. The GCMC simulations used periodic boundary conditions with experimental lattice parameters,^{10c,e} and the excess H₂ amount was calculated as the total amount of H₂ gas contained in the pores minus the amount of the gas that would be present in the pores in the absence of gas–solid intermolecular forces.¹¹ The GCMC simulations used the sorption module of the Cerius2 software.¹⁷

The GCMC simulation used an interatomic FF based on MP2 (second-order Møller–Plesset) ab initio wave functions for H₂ interacting with various fragments of the ZIF. Thus, FF used the Morse functional form to describe the nonbonded interactions such as H₂···H₂ and H₂···ZIFs, because we find that it provides a more accurate inner wall than Lennard-Jones 12–6 or Buckingham exponential-6. We previously developed similar FFs for H₂···H₂, H₂···MOFs, and H₂···COFs (covalent-organic frameworks), where we found excellent agreement with experimental H₂ adsorption isotherms for both MOFs and COFs.^{18,19} In this study we can use four FF terms (H_A···H_A, H_A···C_R, H_A···C₃, and H_A···H_{_}) from our previous FFs. Here H_A designates a hydrogen atom in a H₂ molecule, C_R designates an aromatic carbon atom, C₃ designates an sp³ carbon, and H_{_} designates a hydrogen atom bonded to the carbon. For simulations of H₂ uptake in ZIFs, we require five additional terms: H_A···N_{IM}, H_A···N_{NO₂}, H_A···O_{NO₂}, H_A···Cl, and H_A···Zn. These five terms were based on MP2 calculations with the approximate resolution of the identity (RI-MP2).²⁰ These MP2 calculations were carried out using the Q-CHEM²¹ and TURBOMOLE²² programs. The H_A···N_{IM} term is developed from the interaction between H₂···C₃N₃H₃, the H_A···N_{NO₂} and H_A···O_{NO₂} terms from the interaction between H₂···C₃N₃(NO₂)₃, the H_A···Cl term from the interaction between H₂···C₃N₃Cl₃, and the H_A···Zn term

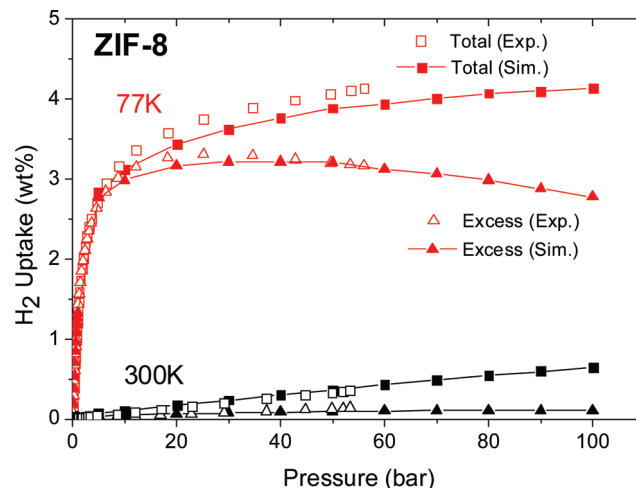


Figure 2. Total and excess H₂ adsorption isotherms of ZIF-8 at 77 (red) and 300 K (black). Here the solid symbols indicate our simulation data and the open symbols reported experimental results. Also, the squares equal total H₂ uptake and the triangles equal excess uptake.

from the interaction between H₂···Zn(NH₂)₄. Detailed information on the development of the FFs can be found in the Supporting Information.

Results and Discussion

Comparison of the Simulated H₂ Adsorption Isotherm with Experiment for ZIF-8. To validate our simulation technique (ab initio based GCMC simulation), we simulated the H₂ adsorption isotherms for ZIF-8 at 77 and 300 K up to 100 bar and compared to experimental¹¹ results (Figure 2).²³ We find excellent agreement between our simulation and experiment for both total and excess isotherms at both of 77 and 300 K well.

For example, at 77 K, our simulation at 1 bar predicts a H₂ uptake value of 1.35 wt % (total) and 1.34 wt % (excess), extremely close to experimental values (total, 1.34 wt %, and excess, 1.32 wt %, at 77 K and 0.97 bar). At a higher pressure (50 bar), our simulation predicts 3.88 wt % (total) and 3.20 wt % (excess), whereas experiment at 49.6 bar indicates 4.06 wt % (total) and 3.20 wt % (excess). Moreover, for high temperature, 300 K, our simulation predictions at 50 bar are 0.36 wt % (total) and 0.09 wt % (excess), whereas the experimental results at 49.89 bar are 0.32 wt % (total) and 0.12 wt % (excess).

This excellent agreement with experimental H₂ loading curves of our GCMC calculations using our first-principles based force field validates our strategy of basing the FF on MP2 QM. The value in a validated first-principles FF is that it might be trusted for materials and conditions not yet explored experimentally.

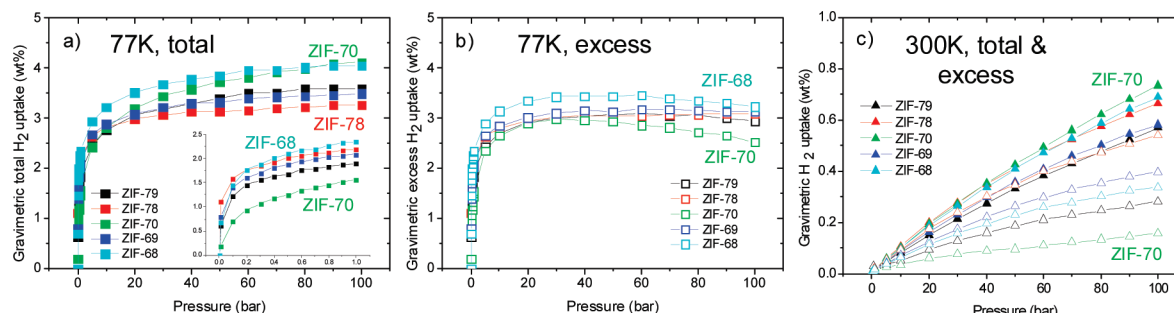


Figure 3. Effects of functional groups in organic linkers of ZIFs on H₂ uptake: (a) simulated total H₂ adsorption isotherms of ZIFs with the GME topology at 77 K up to 100 bar where the inset indicates the total isotherms at low pressure up to 1 bar, (b) simulated excess H₂ adsorption isotherms at 77 K up to 100 bar, and (c) simulated total and excess H₂ adsorption isotherms at 300 K up to 100 bar. Here color codes are cyan = ZIF-68, blue = ZIF-69, green = ZIF-70, red = ZIF-78, and black = ZIF-79.

Effects of Functional Groups in Imidazolate Linkers on H₂ Uptake. To investigate the effect of functional groups, we consider five ZIFs (ZIF-68, ZIF-69, ZIF-70, ZIF-78, and ZIF-79) with the **GME** topology. In ZIF-70, Zn cations are linked through N atoms by two imidazoles, such as IM ($C_3N_2H_3^-$) and nIM ($C_3N_2H_2NO_2^-$), to form neutral frameworks, whereas the ZIF-68 additionally includes a functional group ($-C_6H_4$) in the imidazolate linker, and similarly, the ZIF-69 includes $-C_6H_3Cl$, the ZIF-78 includes $-C_6H_3NO_2$, and ZIF-79 includes $-C_6H_3CH_3$, as represented in Figure 1.

Figure 3 shows the simulated H₂ adsorption isotherms of the five ZIFs with **GME** topology at 77 and 300 K. According to Figure 3a, the highest total H₂ uptake at 77 K and 100 bar occurs in ZIF-70 (4.11 wt %), and the lowest total uptake occurs in ZIF-78 (3.26 wt %). By contrast, at very low pressure (e.g., 10⁻² bar) ZIF-78 has the highest H₂ uptake (1.10 wt %) and ZIF-70 has the lowest value (0.20 wt %), and the sequence of H₂ uptake in all ZIFs is the following: ZIF-78 (1.10 wt %) > ZIF-69 (0.81 wt %) > ZIF-79 (0.69 wt %) > ZIF-68 (0.64 wt %) > ZIF-70 (0.20 wt %). The H₂ uptake at low pressure is determined by the H₂ adsorption energy, which shows a similar trend as is found in MOFs.²⁴ Moreover, the H₂ adsorption energy is decreased with increased pore volume of the ZIFs (Supporting Information Figure S2) because small pores increase the interaction between H₂ and the framework. However, the total H₂ uptake at high pressure depends on the surface area (or pore volume) of ZIFs rather than the H₂ binding energy, where the surface area of ZIF-70 is 1821 m²/g and that of ZIF-78 is 1378 m²/g as given in Table 1.

In Figure 3b, ZIF-68 has an excess H₂ amount of 2.34 wt %, even at 77 K and 1 bar, which is higher than well-known MOFs (e.g., IRMOF-1, 1.15 wt %; IRMOF-6, 1.18 wt %; IRMOF-11, 1.49 wt %; IRMOF-20, 1.28 wt %; MOF-177, 0.98 wt %; MOF-74, 1.34 wt %; HKUST-1, 1.47 wt %)²⁵ and than MOFs that have open metal sites ($Mn_3[(Mn_4Cl)_3(BTT)_8(CH_3OH)_{10}]_2$, 2.23 wt %,²⁵ PCN-9, 1.53 wt %²⁶), which supports the observations that the ZIFs show higher H₂ uptake than the MOFs at low pressure. This high H₂ uptake in ZIFs is caused by the increased H₂ binding energy in the former because of the functional groups and small pore volume relative to the MOFs. The sequence of maximum excess H₂ uptake of ZIFs at 77 K is the following: ZIF-68 (3.46 wt %) at 60 bar > ZIF-69 (3.18 wt %) at 60 bar > ZIF-78 (3.10 wt %) at 90 bar ≈ ZIF-79 (3.10 wt %) at 60 bar > ZIF-70 (2.98 wt %) at 30 bar, which indicates that the maximum excess amount is determined by the surface area of ZIFs except ZIF-70. The relationships between H₂ uptake capacity, surface area, and pore volume will be discussed in detail later.

Although a functional group might increase the H₂ uptake amount at 77 K, this does not guarantee a high H₂ uptake at 300 K. As shown in Figure 3c, all of the ZIFs with **GME** topology show low H₂ uptake of less than 1 wt % even at 100 bar. In addition, it is interesting that among the five ZIFs with GME topology, ZIF-70 has the highest total H₂ uptake at 300 K (or 77 K) and 100 bar; however, it also has the lowest excess uptake under the same conditions. This phenomenon is related to not only the H₂ adsorption energy (Q_{st}) but also the pore volume. Here, the Q_{st} value in ZIFs with GME topology is decreased with increased the pore volume (Supporting Information Figure S2). In other words, the low H₂ adsorption energy in ZIF-70 is because of the absence of the additional aromatic functional group and because of its large pore volume. In comparison with other ZIFs, ZIF-70 has the largest pore volume, which leads to the highest total H₂ uptake. The excess adsorption amount (adsorbed phase) is the absolute amount (adsorbed phase + H₂ bulk gas phase) of gas contained in the pores minus the amount of gas (H₂ bulk gas phase) that would be present in the pores in the absence of gas–solid intermolecular forces. If the H₂ adsorption energy to a ZIF adsorbent is lower for a constant pore volume, the amount of H₂ bulk gas phase is relatively increased. In other words, ZIF-70 has the lowest excess H₂ uptake because the amount of the H₂ bulk gas phase in the ZIF-70 is larger than that in other ZIFs. Moreover, in contrast to other ZIFs, the primary H₂ adsorption site of ZIF-70 is centers of the six-ring-opening channel (Supporting Information Figure S8 and Table S3), not on the organic linkers, which supports the fact that the amount of the H₂ bulk gas phase is larger than for ZIFs.

H₂ Uptake in Other ZIFs. Figure 4 shows the gravimetric and volumetric H₂ uptake of ZIF-2, ZIF-3, ZIF-8, ZIF-10, ZIF-11, and ZIF-70 at 77 and 300 K, where ZIF-70 is included as a representative of the **GME** ZIFs. In Figure 4a, the total gravimetric H₂ uptake amount at 77 K and 100 bar sequence is the following: ZIF-10 (6.72 wt %) > ZIF-3 (6.02 wt %) > ZIF-2 (5.50 wt %) > ZIF-8 (4.13 wt %) > ZIF-70 (4.11 wt %) > ZIF-11 (3.96 wt %). At 77 K and 1 bar the total gravimetric H₂ uptake amount sequence is the following: ZIF-2 (3.11 wt %) > ZIF-3 (2.95 wt %) > ZIF-10 (2.73 wt %) > ZIF-11 (2.39 wt %)²⁷ > ZIF-70 (1.56 wt %) > ZIF-8 (1.35 wt %). Here, the 3.11 wt % of ZIF-2 is similar to the highest H₂ uptake amount (3.05 wt %)²⁸ of PCN-12 with open Cu sites out of the MOFs that have been experimentally reported so far under these conditions. For excess amount at 77 K, the order of the maximum H₂ uptake is the following: ZIF-10 (5.48 wt %) > ZIF-3 (5.28 wt %) > ZIF-2 (5.01 wt %) > ZIF-8 (3.21 wt %) > ZIF-11 (3.17 wt %) > ZIF-70 (2.98 wt %).

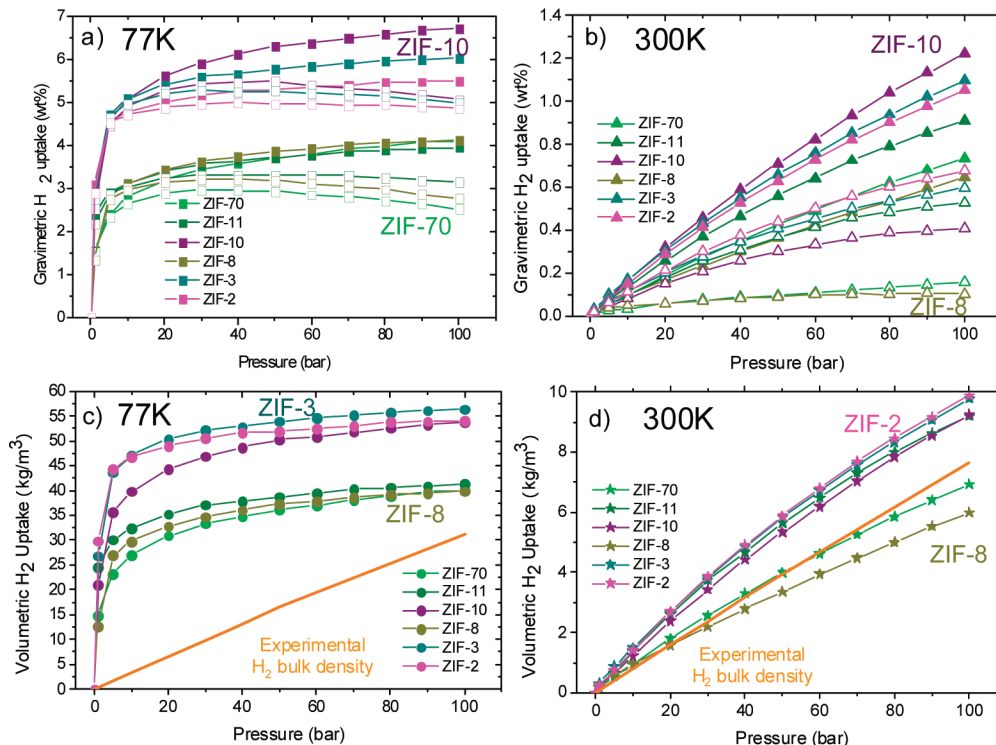


Figure 4. Effects of the ZIF topologies on H₂ uptake: (a) simulated gravimetric total (solid) and excess (open) H₂ adsorption isotherms of ZIFs at 77 K up to 100 bar, (b) simulated gravimetric total (solid) and excess (open) H₂ adsorption isotherms at 300 K up to 100 bar, (c) simulated volumetric total H₂ adsorption isotherms at 77 K up to 100 bar, and (d) simulated volumetric total H₂ adsorption isotherms at 300 K up to 100 bar. Here color codes are pink = ZIF-2, dark cyan = ZIF-3, dark yellow = ZIF-8, purple = ZIF-10, olive = ZIF-11, and green = ZIF-70.

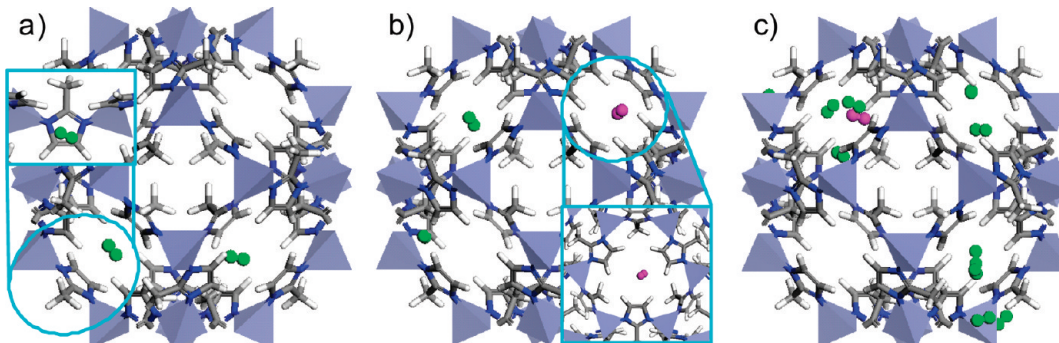


Figure 5. GCMC snapshot for ZIF-8 at 77 K with pressure of (a) 0.1, (b) 0.2, and (c) 0.3 bar. Here, green molecules are H₂ adsorbed on mIM linkers and pink is H₂ located on the center of the six-ring-opening.

At 300 K, both the total and excess H₂ amounts increase with pressure (Figure 4b). The sequence for the total amount of ZIFs at 300 K and 100 bar is ZIF-10 (1.22 wt %) > ZIF-3 (1.10 wt %) > ZIF-2 (1.05 wt %) > ZIF-11 (0.91 wt %) > ZIF-70 (0.74 wt %) > ZIF-8 (0.64 wt %), whereas the sequence for the excess amount at the same conditions is ZIF-2 (0.68 wt %) > ZIF-3 (0.60 wt %) > ZIF-11 (0.53 wt %) > ZIF-10 (0.41 wt %) > ZIF-70 (0.16 wt %) > ZIF-8 (0.10 wt %). The H₂ binding energy is maximized when the pore size of an adsorbent is the same as the kinetic diameter (2.9 Å) of H₂.^{7g} Interestingly, ZIF-11 has a narrow aperture size (3.0 Å), which leads to a high H₂ binding energy. Indeed, ZIF-11 has an initial H₂ binding energy of 15.0 kJ/mol, which will be discussed later. However, the binding energy is not enough to provide high H₂ uptake at room temperature. Accordingly, we find that the ideal pore size (2.9 Å) would not guarantee a high H₂ uptake amount at room temperature due to insufficient H₂ binding energy.

We also investigated volumetric H₂ uptake in ZIFs and then compared them with the experimental free H₂ gas density from

the NIST database²⁹ (Figure 4, parts c and d). At 77 K, the H₂ uptake of all ZIFs is higher than free H₂ density from 0 to 100 bar, whereas at 300 K ZIF-8 shows a lower H₂ uptake than free H₂ density from 20 bar. In other words, ZIF-8 would not store more H₂ compared with an empty H₂ tank, which in fact agrees with an experimental result.¹¹ Similarly, the H₂ density in ZIF-70 is higher than free H₂ up to 60 bar at 300 K; however, the trend is reversed at 60 bar. The order of volumetric H₂ uptake at 77 K and 100 bar is ZIF-3 (56.33 kg/m³) > ZIF-2 (54.08 kg/m³) > ZIF-10 (53.77 kg/m³) > ZIF-11 (41.32 kg/m³) > ZIF-70 (40.04 kg/m³) > ZIF-8 (39.83 kg/m³); the order at 300 K and 100 bar is ZIF-2 (9.89 kg/m³) > ZIF-3 (9.77 kg/m³) > ZIF-10 (9.24 kg/m³) > ZIF-11 (9.20 kg/m³) > ZIF-70 (6.92 kg/m³) > ZIF-8 (6.00 kg/m³).

H₂ Adsorption Sites. Figure 5 presents a GCMC snapshot of ZIF-8 at 77 K to investigate the preferential H₂ adsorption site. Here we observed two different H₂ adsorption sites: the C=C bond in an imidazolate linker and the center of a channel of the six-ring-opening, which is in good agreement with the

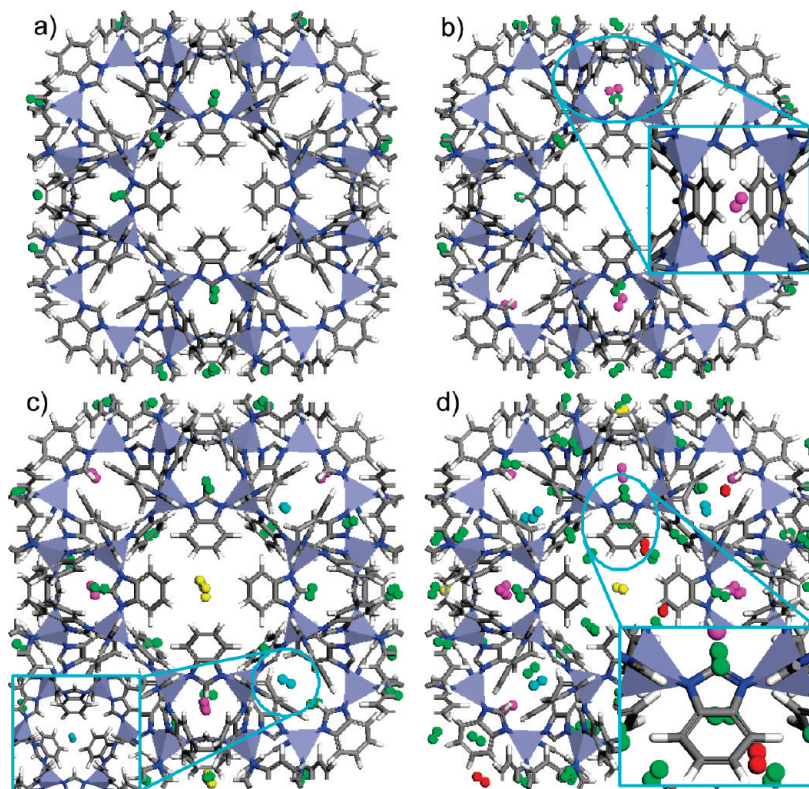


Figure 6. GCMC snapshot for ZIF-11 at 77 K with pressure of (a) 10^{-5} , (b) 5×10^{-5} , (c) 10^{-4} , and (d) 10^{-2} bar. The first preferential H_2 adsorption site (green) is on the five-membered ring of bIM linkers, the second site (pink) is the center of the four-ring-opening channel, the third site (cyan) is the center of the six-ring-opening channel, the fourth site (yellow) is the center of the eight-ring-opening channel, and the fifth site (red) is on the six-membered ring of bIM linkers.

neutron diffraction experiment.¹² At 0.1 bar, H_2 is found only on the $\text{C}=\text{C}$ bond of the linker, which indicates that it is the more preferential H_2 adsorption site. In contrast to the MOFs,³⁰ the primary adsorption site in ZIFs is nearby the imidazolate organic linker, not the ZnN_4 metallic joint, because of the difference in H_2 binding energy. According to our MP2 calculations, the H_2 binding energy to the mIM linker (5.16 kJ/mol) is higher than that to the metallic joint (2.25 kJ/mol); however, in MOF-5, the metallic joint has a higher H_2 binding energy (6.24 kJ/mol) than the organic linker (3.81 kJ/mol).¹⁸ Owing to the steric effect of the $-\text{CH}_3$ group, a H_2 molecule is adsorbed onto the $\text{C}=\text{C}$ bond of the imidazolate linker rather than onto the center of the linker, similar to previous findings.^{12,13}

It is also interesting to clarify the H_2 adsorption sites in ZIF-11 (Figure 6). At 10^{-5} bar, H_2 molecules are preferentially adsorbed on the organic linker, in particular onto the center of the five-membered ring in the linker (Figure 6a). Having the preferential adsorption site be an organic linker is the same as in ZIF-8; however, in ZIF-8 H_2 is adsorbed on the $\text{C}=\text{C}$ bond because of the steric hindrance by $-\text{CH}_3$ group, whereas because ZIF-11 does not include the methyl group, H_2 is adsorbed on the center of the five-membered ring in the bIM linker. Here, the adsorbed H_2 also interacts with the Zn elements of metallic joints, and the H_2 is found on the five-membered ring in the linker rather than on the six-membered ring; moreover, the second preferential adsorption site is the center of the four-ring-opening channel (Figure 6b), the third site is the center of the six-ring-opening channel (Figure 6c), the fourth site is the center of the eight-ring-opening channel (Figure 6c), and the fifth site is on the six-membered ring of the bIM linker (Figure 6d).

In the case of the ZIFs with **GME** topology, we considered ZIF-79 to be a representative of the topology (Figure 7). At

very low pressure (2×10^{-4} bar), H_2 molecules are preferentially adsorbed on the six-membered ring of the organic linker. The organic linker in ZIF-79 is functionalized by the $-\text{C}_6\text{H}_3\text{CH}_3$ group, which leads to a stronger H_2 interaction than the five-membered ring (Figure 7a and Supporting Information Table S1). With increased pressure, H_2 molecules are not only on the six-membered ring but are also sandwiched between four imidazolate linkers in a channel of the four-ring-opening (Figure 7b). Moreover, at 5×10^{-3} bar, H_2 molecules are additionally found on the five-membered ring in the linker as well as in the center of the six-ring-opening (Figure 7c). In other ZIFs with **GME** topology, such as ZIF-68 (Supporting Information Figure S6), ZIF-69 (Supporting Information Figure S7), and ZIF-78 (Supporting Information Figure S9) that are functionalized by $-\text{C}_6\text{H}_4$, $-\text{C}_6\text{H}_3\text{Cl}$, and $-\text{C}_6\text{H}_3\text{NO}_2$, respectively, a similar H_2 adsorption mechanism is observed. However, in the **GME** topology ZIF-70 (Supporting Information Figure S8), the primary adsorption site is at the center of the six-ring-opening, not on the organic linker.

In ZIF-3 (Supporting Information Figure S4) and ZIF-10 (Supporting Information Figure S5), H_2 molecules are preferentially adsorbed in the four-ring-opening channel, in which they are sandwiched between four imidazolate linkers. In ZIF-2 (Supporting Information Figure S3) the preferential adsorption site is the organic linker, where H_2 is coadsorbed on two IM linkers; furthermore, with increased pressure we also find H_2 in centers of the four-, six-, and eight-ring-opening channels. The detailed H_2 adsorption sites in 10 ZIFs are summarized in Supporting Information Table S3.

Relationship between H_2 Uptake and Physical Properties (Isosteric Heat of Adsorption, Surface Area, and Free Volume) of ZIFs. Figure 8a presents the simulated isosteric heat of adsorption (Q_{st}) of ZIFs with total H_2 loading (H_2

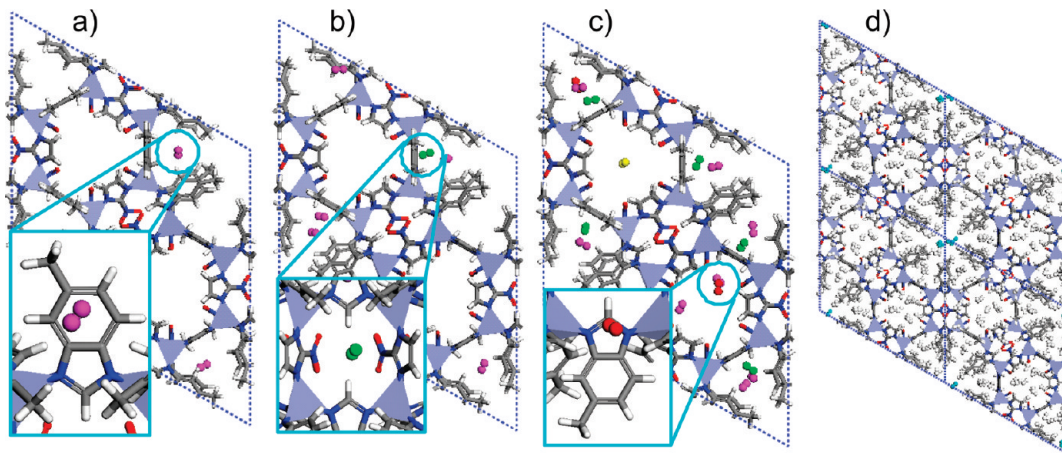


Figure 7. GCMC snapshot for ZIF-79 at 77 K with pressure of (a) 2×10^{-4} , (b) 5×10^{-4} , (c) 5×10^{-3} , and (d) 10^2 bar. The first preferential adsorption site of H₂ (pink) is on the six-membered ring of the mbIM, the second site (green) is the center of four-membered opening channel (sandwiched between four organic linkers), the third site (red) is on the five-membered ring of the mbIM, the fourth site (yellow) is the center of the six-membered opening channel, and the fifth site (cyan) is the center of the twelve-membered opening channel.

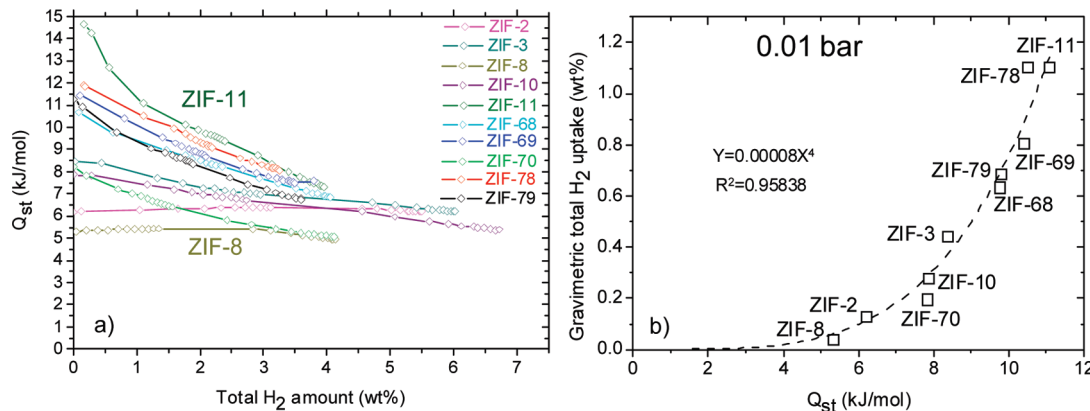


Figure 8. (a) Variation of Q_{st} (kJ/mol) with total H₂ uptake amount (wt %), calculated from the GCMC simulation at 77 K. (b) The relationship between Q_{st} and total H₂ uptake amount at 77 K and 0.01 bar.

pressure) at 77 K.³¹ Among 10 ZIFs considered in this work, ZIF-11 has the highest Q_{st} (~15 kJ/mol) at the initial H₂ loading, where the 15 kJ/mol is higher than 13.5³² kJ/mol for CPO-27-Ni with exposed metal sites, which are the highest yet observed for a MOF. Among considered ZIFs, ZIF-11 has the smallest aperture size (3.0 Å), which is close to the kinetic H₂ diameter (2.9 Å) and thus leads to the maximization of H₂ binding energy.

All ZIFs considered in this work have the four-ring-opening channel, where H₂ binding is increased due to both the small pore size and the sandwich effect between imidazolate linkers around the channel. Of course, they also have 6-, 8-, and/or 12-ring-opening channels. However, the four-ring-opening channel leads to the strongest H₂ binding because it has the smallest pore size. Accordingly, most ZIFs show a preferential H₂ adsorption site nearby the four-ring-opening channel, whereas in ZIF-8 the methyl group of the mIM linker does not allow H₂ to be adsorbed around the four-ring-opening channel because of its steric hindrance. In ZIF-8, H₂ preferentially sits on the C=C bond of mIM linker and the center of six-ring-opening channel (Figure 5). This is the main reason why ZIF-8 has low Q_{st} in comparison with others. On the other hand, an imidazolate linker of ZIF-11 has been additionally functionalized by the $-C_6H_5$ group, which leads to a higher H₂ binding energy (Supporting Information Table S1). With the combination of

small aperture size and the functional group effect, ZIF-11 has the highest Q_{st} .

In Figure 8a, it is also noticeable that the Q_{st} of ZIF-11 is abruptly decreased with H₂ loading because after adsorption around the small aperture, H₂ molecules are stored in large pores of 14.6 Å with increased pressure. Here, it is notable that although the ZIF-11 has a high Q_{st} value, it shows very low H₂ uptake of <1 wt % at room temperature. Therefore, we conclude that a strategy to control pore size (or make appropriate pore size similar to the kinetic diameter of H₂) may not provide the optimum hydrogen storage material.

Second, the GME topology ZIFs (ZIF-68, 69, 78, and 79) with functionalized linkers have high initial Q_{st} values, where ZIF-78 ($-C_6H_3NO_2$) > ZIF-69 ($-C_6H_3Cl$) > ZIF-79 ($-C_6H_3CH_3$) ≈ ZIF-68 ($-C_6H_4$). Then, it is followed by ZIF-3 where H₂ molecules are sandwiched between two five-membered imidazolate linkers, which provides an increase in the H₂ binding energy. Finally, it is followed by ZIF-70, ZIF-2, and ZIF-8, where, interestingly, the Q_{st} in ZIF-2 and ZIF-8 show almost constant values with H₂ loading, which is different from the others. Even at low loading their Q_{st} is slightly increased with H₂ loading, which is attributed to the increased cooperative attraction between adsorbed H₂ molecules, and is consistent with previous simulation on ZIF-8.¹⁴ Also, we need to mention that for ZIF-8 our simulation predicts slightly higher

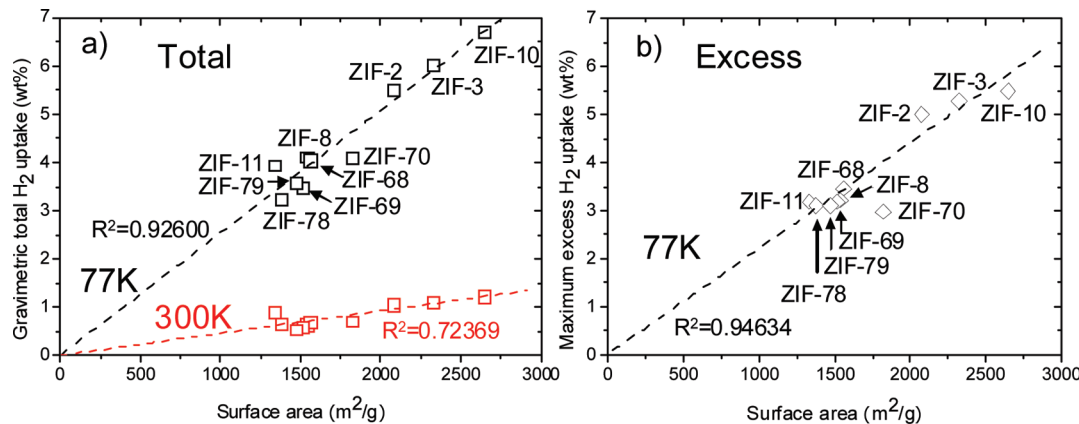


Figure 9. Total H_2 uptake at 100 bar plotted against surface area of ZIFs (a) and the maximum (saturation) excess H_2 uptake plotted against surface area (b).

initial Q_{st} (5.3 kJ/mol) than the experimental value (\sim 4.5 kJ/mol).¹¹ Moreover, the Q_{st} values significantly determine the H_2 uptake at very low pressure (e.g., 0.01 bar), as is shown in Figure 8b.

Figure 9 shows the relationship between maximum H_2 uptake and surface area. Here we find that both the maximum total and excess uptake are correlated with surface area,³³ which is similar to MOFs^{6c} and COFs.³⁴ In particular, in ZIF-70, the maximum excess uptake shows a small deviation from those of other ZIFs because the primary H_2 adsorption site in the ZIF is centers of pores (six-ring-opening channel), not on the organic linkers observed in other ZIFs, shown in Supporting Information Figure S8 and Table S3. Such phenomenon occurs due to large pore size and low adsorption potentials.

Summary

Through GCMC simulations based on an ab initio derived force field, we elucidate the H_2 adsorption mechanism of ZIFs. In comparison with MOFs, the ZIF systems show higher H_2 uptake at low pressure because of their high H_2 binding energies (larger than the highest yet observed for a MOF), which is caused mainly by the small aperture size and by the functional group of the organic linker. The H_2 uptake amount is still lower than the DOE target, as is the case for typical MOFs and COFs. However, ZIFs have superior thermal and chemical stability to the MOFs and COFs. Therefore, to improve H_2 uptake under ambient conditions for practical hydrogen storage, ZIFs could be more versatile in modifying their structure such as alkali-doped ZIFs. Also, similar to MOFs or COFs, the maximum H_2 uptake of ZIFs is determined by their surface area (or pore size) rather than the topology. Nevertheless, H_2 adsorption sites at low loading depend significantly on topology. In particular, the preferential H_2 adsorption site in ZIFs is generally on the organic linker, and not around the metallic joint, which contrasts with typical MOFs. At 77 K, inclusion of the functional group in the imidazolate linker is helpful for improving H_2 uptake at low pressure (e.g., 1 bar) because the H_2 binding energy is increased by an electronic effect of the functional group. However, this does not improve the maximum H_2 uptake at high pressure (e.g., 100 bar) because it decreases the surface area (or pore volume) of ZIFs by its steric effect. Ideally, to obtain high H_2 uptake of ZIFs at both high and low pressures, one should consider ZIFs not only without the functional group for high surface area but also with small pore aperture (e.g., four-ring-opening channel) similar to the kinetic diameter of H_2 by controlling the topology.

Acknowledgment. This research was performed for the Hydrogen Energy R&D Center, one of the 21st Century Frontier R&D programs, funded by the Ministry of Education, Science and Technology of Korea. We thank Accelrys Korea for providing the modeling software. W.A.G. thanks the US-DOE for support (DE-PS36-08GO98004P).

Supporting Information Available: Detailed information on FF development, H_2 uptake amount in all ZIFs, and H_2 adsorption sites in ZIF-2, -3, -10, -68, -69, -70, and -78. This material is available free of charge via the Internet at <http://pubs.acs.org>.

References and Notes

- (1) DOE website. http://www1.eere.energy.gov/hydrogenandfuelcells/storage/current_technology.html (accessed July 4, 2009).
- (2) Seayad, A. M.; Antonelli, D. M. *Adv. Mater.* **2004**, *16*, 765.
- (3) Marder, T. B. *Angew. Chem., Int. Ed.* **2007**, *46*, 8116.
- (4) (a) Han, S. S.; Lee, H. M. *Carbon* **2004**, *42*, 2169. (b) Han, S. S.; Kim, H. S.; Han, K. S.; Lee, J. Y.; Lee, H. M.; Kang, J. K.; Woo, S. I.; van Duin, A. C. T.; Goddard, W. A., III. *Appl. Phys. Lett.* **2005**, *87*, 213113.
- (5) (a) Deng, W. Q.; Xu, X.; Goddard, W. A., III. *Phys. Rev. Lett.* **2004**, *92*, 166103. (b) Han, S. S.; Jang, S. S. *Chem. Commun.* **2009**, 5427.
- (6) (a) Li, H.; Eddaoudi, M.; O'Keeffe, M.; Yaghi, O. M. *Nature* **1999**, *402*, 276. (b) Rosi, N. L.; Eckert, J.; Eddaoudi, M.; Vodak, D. T.; Kim, J.; O'Keeffe, M.; Yaghi, O. M. *Science* **2003**, *300*, 1127. (c) Wong-Foy, A. G.; Matzger, A. J.; Yaghi, O. M. *J. Am. Chem. Soc.* **2006**, *128*, 3494. (d) Kaye, S. S.; Daily, A.; Yaghi, O. M.; Long, J. R. *J. Am. Chem. Soc.* **2007**, *129*, 14176. (e) Frost, H.; Snurr, R. Q. *J. Phys. Chem. C* **2007**, *111*, 18794. (f) Düren, T.; Bae, Y.-S.; Snurr, R. Q. *Chem. Soc. Rev.* **2009**, *38*, 1237. (g) Murray, L. J.; Dincă, M.; Long, J. R. *Chem. Soc. Rev.* **2009**, *38*, 1294. (h) Li, J.-R.; Kuppler, R. J.; Zhou, H.-C. *Chem. Soc. Rev.* **2009**, *38*, 1477. (i) Sumida, K.; Hill, M. R.; Horike, S.; Daily, A.; Long, J. R. *J. Am. Chem. Soc.* **2009**, *131*, 15120.
- (7) (a) Han, S. S.; Goddard, W. A., III. *J. Am. Chem. Soc.* **2007**, *129*, 8422. (b) Han, S. S.; Goddard, W. A., III. *J. Phys. Chem. C* **2008**, *112*, 13431. (c) Blomqvist, A.; Araújo, C. M.; Srepusharawoot, P.; Ahuja, R. *Proc. Natl. Acad. Sci. U.S.A.* **2007**, *104*, 20173. (d) Mavrandonakis, A.; Tylianakis, E.; Stubos, A. K.; Froudakis, G. E. *J. Phys. Chem. C* **2008**, *112*, 7290. (e) Klontzas, E.; Mavrandonakis, A.; Tylianakis, E.; Froudakis, G. E. *Nano Lett.* **2008**, *8*, 1572. (f) Dalach, P.; Frost, H.; Snurr, R. Q.; Ellis, D. E. *J. Phys. Chem. C* **2008**, *112*, 9278. (g) Han, S. S.; Mendoza-Cortés, J. L.; Goddard, W. A., III. *Chem. Soc. Rev.* **2009**, *38*, 1460.
- (8) (a) Mulfort, K. L.; Hupp, J. T. *J. Am. Chem. Soc.* **2007**, *129*, 9604. (b) Mulfort, K. L.; Hupp, J. T. *Inorg. Chem.* **2008**, *47*, 7936.
- (9) Greathouse, J. A.; Allendorf, M. D. *J. Am. Chem. Soc.* **2006**, *128*, 10678.
- (10) (a) Park, K. S.; Ni, Z.; Côté, A. P.; Choi, J. Y.; Huang, R.; Uribe-Romo, F. J.; Chae, H. K.; O'Keeffe, M.; Yaghi, O. M. *Proc. Natl. Acad. Sci. U.S.A.* **2006**, *103*, 10186. (b) Hayashi, H.; Côté, A. P.; Furukawa, H.; O'Keeffe, M.; Yaghi, O. M. *Nat. Mater.* **2007**, *6*, 501. (c) Benerjee, R.; Pahn, A.; Wang, B.; Knobler, C.; Furukawa, H.; O'Keeffe, M.; Yaghi, O. M. *Science* **2008**, *319*, 939. (d) Wang, B.; Côté, A. P.; Furukawa, H.; O'Keeffe,

- M.; Yaghi, O. M. *Nature* **2008**, *453*, 207. (e) Benerjee, R.; Furukawa, H.; Britt, D.; Knobler, C.; O'Keeffe, M.; Yaghi, O. M. *J. Am. Chem. Soc.* **2009**, *131*, 3875.
(11) Zhou, W.; Wu, H.; Hartman, M. R.; Yildirim, T. *J. Phys. Chem. C* **2007**, *111*, 16131.
(12) Wu, H.; Zhou, W.; Yildirim, T. *J. Am. Chem. Soc.* **2007**, *129*, 5314.
(13) Zhou, M.; Wang, Q.; Zhang, L.; Liu, Y.-C.; Kang, Y. *J. Phys. Chem. B* **2009**, *113*, 11049.
(14) Liu, Y.; Liu, H.; Hu, Y.; Jiang, J. *J. Phys. Chem. B* **2009**, *113*, 12326.
(15) Fischer, M.; Hoffmann, F.; Fröba, M. *ChemPhysChem* **2009**, *10*, 2647.
(16) Rankin, R. B.; Liu, J.; Kulkarni, A. D.; Johnson, J. K. *J. Phys. Chem. C* **2009**, *113*, 16906.
(17) The Cerius2 Software, version 4.10; Accelrys Inc.: San Diego, CA, 2005.
(18) Han, S. S.; Deng, W. Q.; Goddard, W. A., III. *Angew. Chem., Int. Ed.* **2007**, *46*, 6289.
(19) Han, S. S.; Furukawa, H.; Yaghi, O. M.; Goddard, W. A., III. *J. Am. Chem. Soc.* **2008**, *130*, 11580.
(20) (a) Weigend, F.; Häser, M. *Theor. Chem. Acc.* **1997**, *97*, 331. (b) Ahlrichs, R.; Bär, M.; Häser, M.; Horn, H.; Kölmel, C. *Chem. Phys. Lett.* **1989**, *162*, 165.
(21) Q-CHEM Software, version 3.2; Q-Chem Inc.: Pittsburgh, PA, 2007.
(22) TURBOMOLE Software, version 5-7; University of Karlsruhe: Karlsruhe, Germany, 2004.
(23) Two experimental studies (refs 10a and 11) for H₂ uptake in ZIF-8 have been reported. However, these two experiments lead to different H₂ uptake behavior. For example, at 77 K and 20 bar, ref 10a finds 2.77 wt % H₂ while ref 11 finds 3.26 wt %. Such a discrepancy in the experimental H₂ uptake amount might result from a difference in pore volume or surface area (perhaps due to residual solvent of incomplete reactions). This was

explained in a recent simulation study (ref 13). Our simulations are closer to ref 11. For example, at 77 K and 20 bar we find 3.16 wt %.

(24) Frost, H.; Düren, T.; Snurr, R. Q. *J. Phys. Chem. B* **2006**, *110*, 9565.

(25) Dincă, M.; Long, J. R. *J. Am. Chem. Soc.* **2007**, *129*, 11172.

(26) Ma, S.; Zhou, H.-C. *J. Am. Chem. Soc.* **2006**, *128*, 11734.

(27) Our GCMC result for ZIF-11 shows higher H₂ uptake at low pressure (<1 bar) in comparison to an experimental result (ref 10a). Such discrepancy could be generated by the difference of pore volume or surface area of the synthesized ZIF. In the reference, the experimental pore volume and surface area were not reported because the aperture size (3.0 Å) of ZIF-11 is smaller than the kinetic diameter (3.6 Å) of N₂.

(28) Wang, X.-S.; Ma, S.; Forster, P. M.; Yuan, D.; Eckert, J.; López, J. J.; Murphy, B. J.; Parise, J. B.; Zhou, H.-C. *Angew. Chem., Int. Ed.* **2008**, *47*, 7263.

(29) NIST website. <http://webbook.nist.gov/chemistry/fluid> (accessed June 1, 2006).

(30) Yildirim, T.; Hartman, M. R. *Phys. Rev. Lett.* **2005**, *95*, 215504.

(31) In calculating the Q_{st} , we employ the fluctuation formula, $Q_{st} = k_B T - \{\langle NU \rangle - \langle N \rangle \langle U \rangle\} / \{\langle N^2 \rangle - \langle N \rangle \langle N \rangle\}$, where N and U are the number of H₂ and the total internal energy in any given configuration, respectively, and $\langle \cdot \rangle$ represents a configuration average (ref 19).

(32) Vitillo, J. G.; Regli, L.; Chavan, S.; Ricchiardi, G.; Spoto, G.; Dietzel, P. D. C.; Bordiga, S.; Zecchina, A. *J. Am. Chem. Soc.* **2008**, *130*, 8386.

(33) We also investigated the relationship between maximum total H₂ uptake and pore volume and found that the maximum H₂ uptake correlates better with surface area than pore volume. This phenomenon is also maintained at 150 bar.

(34) Furukawa, H.; Yaghi, O. M. *J. Am. Chem. Soc.* **2009**, *131*, 8875.

JP103785U